ACS APPLIED MATERIALS & INTERFACES

Research Article

www.acsami.org

# Reversible Superhydrophilicity and Superhydrophobicity on a Lotus-Leaf Pattern

Al de Leon and Rigoberto C. Advincula*

Department of Macromolecular Science and Engineering, Case Western Reserve University, Cleveland, Ohio 44106, United States

Supporting Information

**ABSTRACT:** A facile approach of fabricating a temperature-responsive coating capable of switching reversibly from being superhydrophobic to superhydrophilic is presented. The approach combines micromolding, layer-by-layer assembly of the polymer macroinitiators, and surface-initiated polymerization. Changing between superhydrophobicity and superhydrophilicity depends heavily on the surface roughness and the switching of the surface energy levels. In this study, surface roughness was introduced by replicating the surface morphology of a lotus leaf. The switching of surface energy levels was made possible by grafting a temperature-responsive polymer brush. Wetting studies reveal that the reported approach not only replicates nature but also improves its property by making it responsive to stimulus.

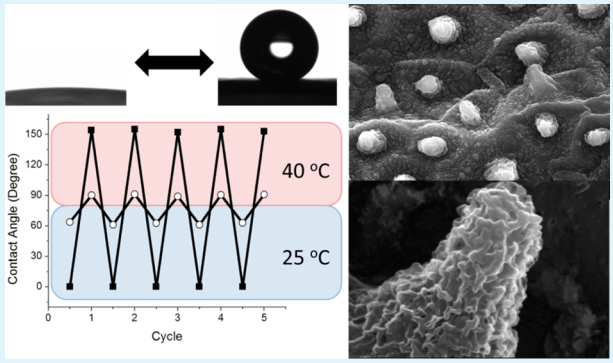


**KEYWORDS:** *superhydrophobic, superhydrophilic, stimuli-responsive, nature-inspired, biomimetics*

## INTRODUCTION

Biomimetics involves not only the study of biological materials, both of its structures and functions, but also the use of principles attained from nature in developing systems that mimic it.[1] For some applications copying nature is not enough. Mimicking nature and incorporating another property, i.e., making it stimuli-responsive, can vastly widen the application of the material being developed. Recently, the modification of the surface to impart a stimuli-responsive behavior is gaining a lot of attention in developing functional coatings for drug delivery and as biomimetic materials, among others.[2−4] Of particular interest is the reversible switching between superhydrophobicity and superhydrophilicity.[5,6] The wetting property of the surface depends heavily on its surface energy and on its surface roughness. One of the most effective ways of controlling the surface energy (and surface roughness to some extent) is by covalently grafting polymer chains on the surface.[7] The surface characteristic imparted by these high-density surface-tethered polymer chains, more popularly known as polymer brush, depends on what polymer is used. A lot of research has been focusing on using stimuli-responsive polymer brushes as coatings. Stimuli that have been used to trigger the change in property of the surface include, but not limited to, temperature, electrical potential, and light.[8−10]

Poly(*N*-isopropylacrylamide) (PNIPAM) is one of the most studied temperature-responsive polymers because of its lower critical solution temperature (LCST) at about 32 °C.[11−14] At temperatures below the LCST, the polymer chains are extended away from the surface and the −C═O and −N−H functional groups are hydrogen-bonded to water molecules. On the other hand, at temperatures above the LCST, the polymer chains are collapsed and compact, the water molecules are expelled, and predominately intramolecular hydrogen-bonding exists between the polar functional groups. The transition from extended-to-collapsed configuration of PNIPAM is accompanied by a significant change in surface free energy. When the polymer brush is extended, the polar groups are exposed at the surface, and thus the surface free energy is high. In contrast, when the polymer chain is collapsed, the nonpolar polymer backbones are exposed on the surface, and thus the surface energy is low. Surface free energy has a major impact on the wettability of the surface: surfaces with low free energy are hydrophobic (contact angle greater than 90°), while surfaces with high free energy are hydrophilic (contact angle less than 90°).[15]

Surface roughness can enhance the surface's wetting property as implied by the Wenzel Model and the Cassie−Baxter Model.[16,17] By incorporating dual-scale roughness and introducing heterogeneity on the surface energy, hydrophilic surfaces can become superhydrophilic (contact angle about 0°), while hydrophobic surfaces can become superhydrophobic (contact angle greater than 150°). Because of the temperature-driven switching between high and low surface energies, PNIPAM has been used to demonstrate the reversible switching between superhydrophobicity and superhydrophilicity. Recently, PNIPAM was electrospun with polystyrene and the fabricated nanofibers are thermally responsive.[18] The

**Received:** October 3, 2014
**Accepted:** November 20, 2014
**Published:** November 20, 2014





dx.doi.org/10.1021/am506050k | *ACS Appl. Mater. Interfaces* 2014, 6, 22666−22672

**Scheme 1. Fabrication Scheme of the Temperature-Responsive Surface with Lotus-Leaf Morphology**

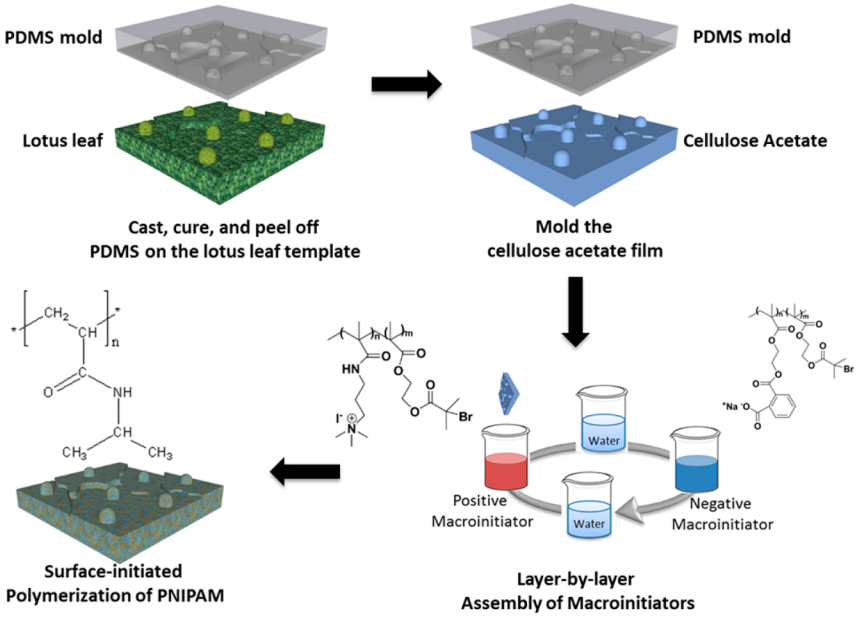


procedure was proven to be low-cost and facile; however, the need for electrospinning may limit its application.

An alternative approach for introducing roughness is to imprint patterns on a polymer coating. The patterned polymer coating can act as the base for the stimuli-responsive polymer brush. Several approaches, such as a technique called solvent-assisted micromolding (SAMIM), for imprinting patterns have been studied.[19] SAMIM imprints the pattern on a polymer film softened by a suitable solvent with a soft polymeric mold. With this approach, surface roughness can be introduced to a wide variety of polymers coated on any substrate like glass, silicon wafer, and steel. SAMIM can be used to replicate surface features of materials existing in nature. Many biological materials exhibit excellent wetting properties brought about by their dual-scale structures and low surface energy coating. Lotus plant, for instance, contains micropapillae decorated with nanofeatures. Because this hierarchical structure is coated with a waxy material, the lotus plant leaf exhibits superhydrophobic and self-cleaning properties.[20,21] Mimicking the surface morphology of the lotus leaf can be a very effective way of introducing surface features on stimuli-responsive polymer systems.

Initiators for polymerization can be introduced to the replicated polymer film via self-assembly, or through a series of chemical reactions.[22] If the molded polymer film bears a charge, then a layer-by-layer (LbL) assembly of initiators can be employed. Layer-by-layer assembly is the alternating deposition of oppositely charged materials on a substrate or on a particle. The main driving force is the electrostatic attraction between the charges.[23] Layer-by-layer assembly and the subsequent surface-initiated polymerization (LbL-SIP) have been established to be a very promising method for the synthesis of very dense and stimuli-responsive coatings. The Advincula group has utilized LbL-SIP to fabricate solvent- and temperature-responsive thin-film coatings, and freestanding films.[24,25] We were successful in grafting homopolymer, block copolymer, and mixed polymer brushes on the surface prefunctionalized via layer-by-layer assembly of macroinitiators. Effects of solvent and temperature on properties like thickness and morphology of these polymer brushes were also studied. To release the free-standing film, we either dissolved the cellulose acetate sacrificial layer, or spin-casted poly(vinyl alcohol) on top of the polymer brush, physically peeled it off, and dissolved the poly(vinyl alcohol). The response of the free-standing films to change in pH, temperature, and solvent were then studied.

In this study, we used SAMIM to replicate the lotus-leaf surface morphology on a thin cellulose acetate film coated on glass. We then deposited polyelectrolyte macroinitiators via layer-by-layer assembly and polymerized PNIPAM via atom transfer radical polymerization. Reversible switching between superhydrophobicity and superhydrophilicity was then demonstrated. The fabrication method reported here should be applicable to copy and to improve a wide variety of naturally existing morphologies. To our knowledge, this is the first study to combine SAMIM, layer-by-layer assembly of macroinitiators, and surface-initiated polymerization in fabrication of stimuli-responsive polymer coating.

## RESULTS AND DISCUSSION

Fabrication of the temperature-responsive surface by replication of the surface morphology of the lotus leaf, deposition of the macroinitiators, and growth of polymer brush is illustrated in Scheme 1. Briefly, uncured polydimethylsiloxane (PDMS) solution was casted on a fresh lotus leaf. The solution was cured at 50 °C for 2 h. The cured PDMS, which bears the negative replica of the lotus-leaf surface, was peeled off. The cured PDMS was used to mold the cellulose acetate film, which is coated on a glass substrate and is softened by acetone. Cellulose acetate in aqueous solution is negatively charged because of the partial hydrolysis of the ester group as evidenced by its negative zeta potential in pH range of 2−10.[26] Positively and negatively charged macroinitiators (structures shown in the scheme) were deposited via layer-by-layer assembly on top of the partially negatively charged cellulose acetate. The macroinitiators used in this study were synthesized previously in our laboratory. Details of the synthesis are available elsewhere.[27]

Successful replication of the surface of the lotus leaf can be confirmed by comparing the images captured using a scanning

electron microscope (SEM) of the template (Figure 1a) and the replicated surface after growing the PNIPAM brush (Figure 1b). The diameter of the base of the micropapillae ranges from 3 to 8 $\mu$m. Figure 1c shows that the lotus-leaf morphology was replicated on a large area. Higher magnification view of the micropappilae reveals that the microstructures are decorated with nanoscale cilium-like structures (Figure 1d).[28] The combination of micro- and nanoscale roughness renders the surface superhydrophobic or superhydrophilic depending on its surface energy.

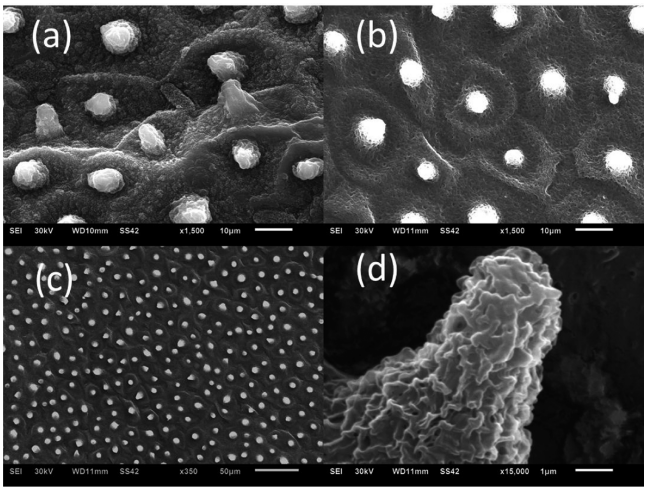


**Figure 1.** SEM images of the (a) lotus-leaf template (1500×), (b) replicated surface after growth of PNIPAM brush (1500×), (c) wide-area image of the replicated surface (350×), and (d) high-magnification image of the micropapillae (15000×).

Figure 2a shows the reversible thermal response of both the flat and the replicated surface as captured by the CCD camera. For the flat surface, the contact angle is measured to be 62° ± 2° at 25 °C. Increasing the temperature to 40 °C increased the contact angle to 90° ± 1°. As the film is cooled back to 25 °C, the contact angle decreased back to 61° ± 1°. The reversible switching was continued for four more cycles (Figure 2b). The switching only happens between about 62° and 90°, which indicates the chemical nature of the PNIPAM brush is not altered during the temperature changes. The switching from hydrophilic to hydrophobic is brought about by the change in chain configuration of the polymer as water is drove off. PNIPAM is known to have lower critical solution temperature (LCST) of about 32 °C.[25] Below the LCST, the PNIPAM is predominantly hydrogen-bonded to water molecules, which causes the surface to be hydrophilic. The high surface energy is brought about by the availability of strong polar groups, like C═O and N−H, to interact with the environment. Above the LCST, the hydrogen bonding is predominantly intramolecular; i.e., the bonding is between the C═O and N−H groups of PNIPAM. This results in the collapsed conformation of the polymer chain and effectively exposing the low surface energy hydrocarbon backbone of the polymer brush. This also makes it difficult for water to interact with the hydrophilic C═O and N−H, and as a result making the surface hydrophobic.

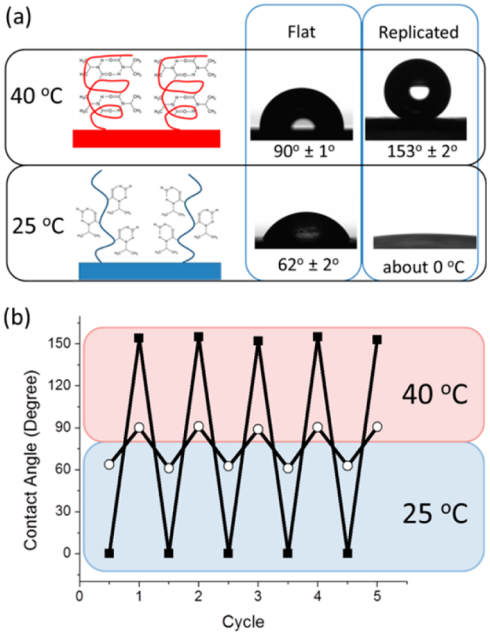


**Figure 2.** (a) Effect of temperature on the wettability, and (b) reversibility study of thermal switching of surface wettability of flat (○) and replicated surfaces (■).

The thermal response of the surface is enhanced dramatically for the replicated surface. At temperature below the LCST, the surface is superhydrophilic (contact angle of 0°), while at a temperature above the LCST, the surface is superhydrophobic (contact angle of 153° ± 2°). The advancing ($\theta_{adv}$) and receding angles ($\theta_{rec}$) were also measured to be 155° ± 1° and 151° ± 1°, respectively. With a very low hysteresis of about 4°, the film is expected to exhibit self-cleaning effect. The self-cleaning phenomenon is confirmed by dropping a small volume of water on an inclined coated surface (Figure S1, Supporting Information). The water droplet rolled off the surface when the surface was tilted at a very small sliding angle of ∼2°. The contact angle of a hydrophobic film can be significantly increased by making the surface rougher as implied by the Wenzel and the Cassie−Baxter Models.[16] The superhydrophobic/superhydrophilic property depends strongly on the surface roughness and surface energy.[29] For this system, surface roughness was introduced by using cellulose acetate molded to replicate the surface of a lotus leaf. As seen on the SEM images, the cellulose acetate provides the microscale roughness, while the macroinitiator layers and the PNIPAM brush provide the majority of the nanoscale roughness and the surface energy. Air is believed to be trapped between the micro- and nanostructures and is the reason for minimal contact between the water droplet and the surface.[30] This causes the hydrophobic surface to be superhydrophobic. On the other hand, 3D and 2D capillary effect, also brought about by the hierarchical structure, causes the hydrophilic surface to be superhydrophilic.[31]

The surface roughness for both flat and replicated surfaces can be quantified by using atomic force microscopy (AFM). Figure S2 compares the 3D AFM images of the flat and the replicated surfaces. For the flat surface, the measured average feature height is 51.5 and 141.4 nm, before and after the surface-initated polymerization of PNIPAM, respectively. This is also accompanied by a change in roughness from 14.7 nm (before polymerization) to 67.8 nm (after polymerization). In comparison, the average feature height for the replicated surface is 3.019 $\mu$m and the roughness is 1.304 $\mu$m. The significant increase in surface roughness contributes to the super-

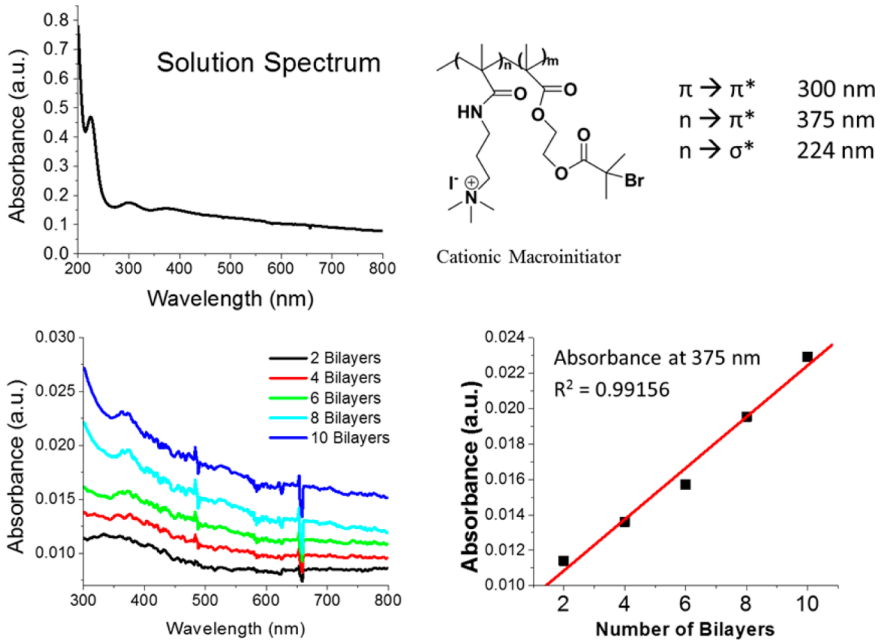


**Figure 3.** (a) UV−vis spectrum of the cationic macroinitiator. (b,c) Multilayer growth of the LbL tracked by UV−vis.

hydrophobic/superhydrophilic property of the replicated surface in comparison to the flat surfaces.

Deposition of the macroinitiators on the molded cellulose acetate film was monitored by using UV−vis spectroscopy. Figure 3a shows the absorbance from 200 to 800 $cm^{-1}$ of the cationic macroinitiator. Three relevant peaks are observed: at 375 nm, which corresponds to the $\pi \rightarrow \pi^*$ transition; at 300 nm, which corresponds to the n $\rightarrow \pi^*$ transition; and at 224 nm, which corresponds to the n $\rightarrow \sigma^*$ transition. Figure 3b shows the UV−vis spectrum (from 300 to 800 $cm^{-1}$) for every two bilayers of the macroinitiators deposited on the molded cellulose acetate. As expected, the absorbance increases with the amount of deposited macroinitiators. The absorbance at 375 nm was plotted against the number of macroinitiator bilayers (Figure 3c). The resulting graph shows a linear dependence between the absorbance and the number of macroinitiator bilayers, signifying that the amount of macroinitiator increases linearly as the number of bilayers is increased. This further confirms the successful deposition of macroinitiators on the molded cellulose acetate.

X-ray photoelectron spectroscopy (XPS) was used to determine the elemental composition of film. The survey scan for the cellulose acetate, as shown in Figure 4a, contains only the signals for carbon (C) and oxygen (O). In the same figure, we can see that C, O, nitrogen (N), and bromine (Br) are present for the macroinitiator layers and for PNIPAM brush. By getting the area under the peaks for N and O, we can get the relative amount of N and O (i.e., N/O) of the three samples. Since there is no nitrogen in cellulose acetate, the N/O ratio is 0. For the macroinitiator, the ratio is 0.11. Looking at the structures of the macroinitiators, we can see that there are approximately 2 N's for every 15 O's, and the N/O ratio is equal to 0.13. After the polymerization of PNIPAM, the N/O increased to 0.95. This means that there is 1 O for every N, which is consistent with the structure of PNIPAM. Also, the signal for Br is still present for PNIPAM, confirming the living nature of the polymerization.[24] The absence of the peak at

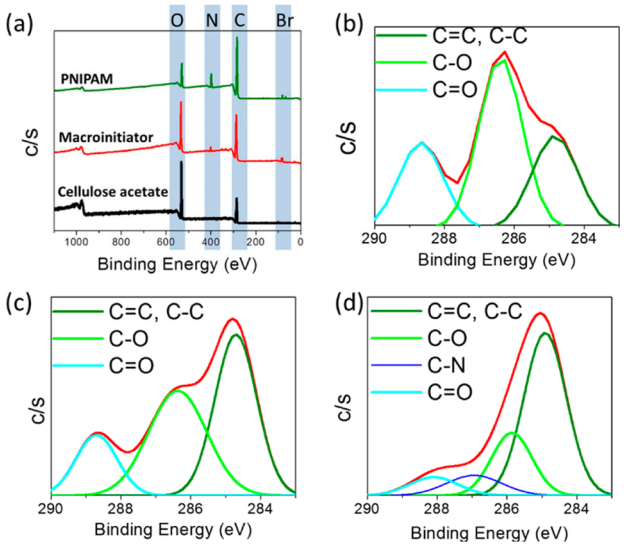


**Figure 4.** (a) XPS survey scan and high-resolution carbon scan of the cellulose acetate film (b), after LbL assembly of macroinitiators (c), and after the growth of PNIPAM brush (d).

~950 eV indicates that there is no copper catalyst left on the PNIPAM surface.

Additional information can be gained by analyzing the high-resolution carbon scan for each sample. Figure 4b shows that the cellulose acetate contains C−C (and C═C) at 284.71 eV, C−O at 286.37 eV, and C═O at 288.70 eV,[31] which is consistent with the structure of cellulose acetate. The same set of peaks are observed for the macroinitiators. Take note that C−N and C−Br bonds do not appear probably because their contribution is negligible compared to the other oxidation states of carbon. After the polymerization of PNIPAM, the C−N peak intensity becomes more significant. The presence of C−O indicates that, on some areas, the macroinitiator layers are still within 5−10 nm depth and are detectable by XPS.

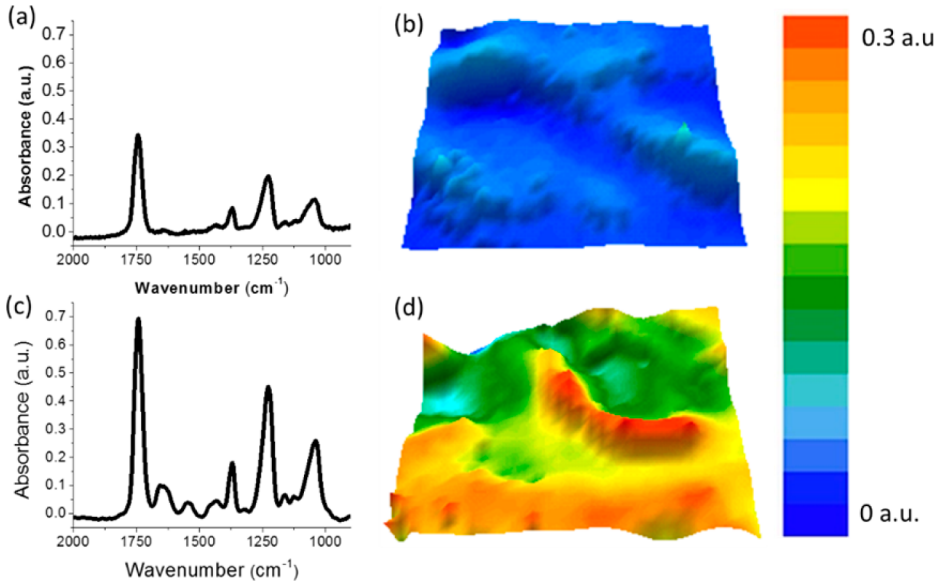


**Figure 5.** FT-IR spectrum and FT-IR images (focused at 1650 $cm^{-1}$) of the molded cellulose acetate (a,b) and after growing the PNIPAM brush (c,d), respectively. Area is 176 × 176 $\mu$m.

Fourier transform infrared spectroscopy (FTIR) was also utilized to further confirm the successful growth of the PNIPAM brush on the molded cellulose acetate. For the cellulose acetate (Figure 5a) the relevant peaks are 3580−3650 $cm^{-1}$ for the hydrogen-bonded O−H stretching, 2850−3000 $cm^{-1}$ for C−H stretching, 1740 $cm^{-1}$ for the ester C═O, 1220 and 1040 $cm^{-1}$ for the C−O stretches, and 1370 $cm^{-1}$ for the C−H bending. Upon growth of the PNIPAM brush on the molded cellulose acetate, new peaks at 1650 $cm^{-1}$, which corresponds to C═O stretch (amide I), and at 1545 $cm^{-1}$, which corresponds to N−H bending (amide II band), are observed (Figure 5c).[24] FTIR imaging was also utilized to check the surface coverage of the PNIPAM brush. Figure 5b,d shows the IR images of cellulose acetate and PNIPAM brush, respectively, focused at 1650 $cm^{-1}$. As expected, the absence of amide C═O stretching causes very low absorbance at 1650 $cm^{-1}$ for cellulose acetate. On the other hand, intense absorption at 1650 $cm^{-1}$ was observed for PNIPAM brush.

## CONCLUSION

In this study, we demonstrated that the stimuli-responsive polymer brush could be grown from a multilayer film of macroinitiators deposited on top of the cellulose acetate coating replicated from a lotus leaf. The polymer coating shows reversible switching between superhydrophobicity and superhydrophilicity even after five cycles of heating and cooling. This reversible switching is made possible by the temperature-driven changing of the surface energy levels of the PNIPAM brush. The approach is proven to not only replicate nature but also to improve its property by making it stimuli-responsive. In addition, the nonspecificity and facileness of the coating procedure may prove advantageous in imparting reversible stimuli-responsive wetting on any substrate.

## EXPERIMENTAL SECTION

**Preparation of the PDMS Mold.** The uncured PDMS solution was prepared by mixing 10 parts of elastomer base and 1 part curing agent (Sylgard 184, Dow Corning). The PDMS solution was poured on the fresh lotus leaf and then cured at 50 °C for 2 h. After curing, the PDMS mold was peeled off gently from the lotus leaf and was used as the negative template.

**Fabrication of the Replicated Surface.** Glass substrates were cut into 2.5 cm × 1.5 cm sizes, cleaned by sonication in piranha solution (30% of 30% $H_2O_2$/70% concentrated sulfuric acid) for 20 min, in Milli-Q water (18.2 MΩ-cm resistivity) for 20 min, and then in acetone for 20 min, and finally cleaned by oxygen plasma for 3 min. Five weight percent of cellulose acetate was spin-casted on silicon wafer at 3000 rpm for 60 s. The PDMS mold was placed on the cellulose acetate (Aldrich) softened by acetone for 20 min. The mold was removed after all the acetone has evaporated. The negatively charged substrate was then immersed automatically by a programmable dipping machine (HMS Series Programmable Slide Stainer, Carl Zeiss, Inc.) alternately to positive and negative macroinitiator solutions for 20 min per layer with washing in Milli-Q water in between. The concentration of both macroinitiators is 1 mg/mL. Ten bilayers of macroinitiators were deposited.

**Surface-Initiated Polymerization.** For PNIPAM, monomer solution was prepared by mixing 1 g of *N*-isopropylacrylamide (>98% TCI America, recrystallized in *n*-hexane to remove the initiator), 60 $\mu$L of *N*,*N*,*N*′,*N*′,*N*″-pentamethyldiethylenetriamine (PMDETA, 99% Aldrich), 9 mL of Milli-Q water, and 9 mL of methanol in a 20 mL vial. The solution was degassed to remove dissolved oxygen and impurities for 1 h. The solution was then transferred to another vial containing 12.7 mg of Cu(I)Br (98% Alfa Aesar, also degassed) via a cannula. The green solution was transferred to another vial containing the replicated surface with macroinitiators. The polymerization was conducted at room temperature and with slight overpressure of nitrogen to prevent oxygen from prematurely terminating the reaction. After 1 h, the solution was exposed to air and the functionalized surface was washed with a generous amount of water to remove the unreacted monomer, the catalyst, and the ligand.

**Instrumentation.** Static and dynamic water contact angles were measured by using a CAM 200 optical contact angle meter (KSV Instruments Ltd.). SEM analysis was done using JEOL JSM-6510LV SEM. FT-IR imaging was conducted on a

Digilab FTS 7000 spectrometer, a UMA 600 microscope, and a 32 × 32 MCT IR imaging focal plane array image detector with an average spatial area of 176 $\mu$m × 176 $\mu$m in the reflectance mode. XPS data (at takeoff angle of 45° from the surface) was recorded using a PHI 5700 X-ray photoelectron spectrometer with a monochromatic Al K$\alpha$ X-ray source ($h\nu$ = 1486.7 eV) incident at 90° relative to the axis of hemispherical energy analyzer. High-resolution carbon spectra were curve-fit using Gaussian−Lorentzian functions with a Shirley background correction. All atomic force microscopy images were recorded using a PicoScan System (Agilent Technologies, formerly Molecular Imaging Corp.) with 8 $\mu$m × 8 $\mu$m scanner. Tapping mode was used for all samples. UV−vis spectra were obtained by using an Agilent 8453 spectrometer.

## ■ ASSOCIATED CONTENT

### Supporting Information

Figure S1 shows the movement of the water droplet on the surface inclined at a very low sliding angle of ∼2°. Figure S2 shows the 3D AFM images of (a) a flat surface with layer-by-layer assembled macroinitiators, (b) flat surface after the surface-initiated polymerization of PNIPAM, and (c) replicated surfaces after the surface-initiated polymerization of PNIPAM. This material is available free of charge via the Internet at http://pubs.acs.org.

## ■ AUTHOR INFORMATION

### Corresponding Author

*E-mail: rca41@case.edu. Phone: 216-368-4566.

### Notes

The authors declare no competing financial interest.

## ■ ACKNOWLEDGMENTS

We acknowledge Dr. Nicel Estillore for the preparation and synthesis of the macroinitiator. We gratefully acknowledge funding from NSF EAGER CHE-1247438, NSF-STC-0423914, and DMR-1304214 and technical support from Malvern (Viskotek), Biolin, Agilent Technologies, and Park Systems.

## ■ REFERENCES

(1) Vincent, J.; Bogatyreva, O.; Bogatyrev, N.; Bowyer, A.; Pahl, A. Biomimetics: Its Practice and Theory. *J. R. Soc. Interface* **2006**, *22*, 471−482.

(2) Sun, T.; Feng, L.; Gao, X.; Jiang, L. Bioinspired Surfaces with Special Wettability. *Acc. Chem. Res.* **2005**, *38*, 644.

(3) Shi, F.; Song, Y.; Niu, J.; Xia, X.; Wang, Z.; Zhang, X. Facile Method To Fabricate a Large-Scale Superhydrophobic Surface by Galvanic Cell Reaction. *Chem. Mater.* **2006**, *18*, 1365.

(4) Liu, Y.; Mu, L.; Liu, B.; Kong, J. Controlled Switchable Surface. *Chem.—Eur. J.* **2005**, *11*, 2622.

(5) Yang, J.; Zhang, Z.; Men, X.; Xu, X.; Zhu, X. Reversible Superhydrophobicity to Superhydrophilicity Switching of a Carbon Nanotube Film via Alternation of UV Irradiation and Dark Storage. *Langmuir* **2010**, *26*, 10198−10202.

(6) Liu, H.; Feng, L.; Zhai, J.; Jiang, L.; Zhu, D. Reversible Wettability of a Chemical Vapor Deposition Prepared ZnO Film between Superhydrophobicity and Superhydrophilicity. *Langmuir* **2004**, *20*, 5659−5661.

(7) Stratakis, E.; Mateescu, A.; Barberoglou, M.; Vamvakaki, M.; Fotakis, C.; Anastasiadis, S. From Superhydrophobicity and Water Repellency to Superhydrophilicity: Smart Polymer-functionalized Surfaces. *Chem. Commum.* **2010**, *46*, 4136−4138.

(8) Jiang, W.; Wang, G.; He, Y.; Wang, X.; An, Y.; Song, Y.; Jiang, L. Photo-switched Wettability on an Electrostatic Self-assembly Azobenzene Monolayer. *Chem. Commun.* **2005**, *28*, 3550.

(9) Fu, Q.; Rao, G.; Basame, S.; Keller, D.; Artyushkova, K.; Fulghum, J.; Lopez, G. Reversible Control of Free Energy and Topography of Nanostructured Surfaces. *J. Am. Chem. Soc.* **2004**, *126*, 8904.

(10) Riskin, M.; Basnar, B.; Chegel, V.; Katz, E.; Willner, I.; Shi, F.; Zhang, X. Switchable Surface Properties Through the Electrochemical or Biocatalytic Generation of Ag0 Nanoclusters on Monolayer-Functionalized Electrodes. *J. Am. Chem. Soc.* **2006**, *128*, 1253.

(11) Chang, D. P.; Dolbow, J. E.; Zauscher, S. Switchable Friction of Stimulus-Responsive Hydrogels. *Langmuir* **2007**, *23*, 250−257.

(12) Kim, J. H.; Lee, T. R. Discrete Thermally Responsive Hydrogel-Coated Gold Nanoparticles for Use as Drug-Delivery Vehicles. *Drug Dev. Res.* **2006**, *67*, 61−69.

(13) Balamurugan, S.; Mendez, S.; Balamurugan, S. S.; O'Brien, M. J.; Lopez, G. P. Thermal Response of Poly(N-isopropylacrylamide) Brushes Probed by Surface Plasmon Resonance. *Langmuir* **2003**, *19*, 2545−2549.

(14) Ista, L. K.; Mendez, S.; Perez-Luna, V. H.; Lopez, G. P. Synthesis of Poly(N-isopropylacrylamide) on Initiator-Modified Self-Assembled Monolayers. *Langmuir* **2001**, *17*, 2552−2555.

(15) Owens, D. K.; Wendt, R. C. Estimation of the Surface Free Energy of Polymers. *J. Appl. Polym. Sci.* **1969**, *13*, 1741−1747.

(16) Wenzel, R. N. Resistance of Solid Surfaces to Wetting by Water. *Ind. Eng. Chem. Res.* **1936**, *28*, 988−994.

(17) Cassie, A. B. D.; Baxter, S. Wettability of Porous Surfaces. *Trans. Faraday Soc.* **1944**, *40*, 546.

(18) Wang, N.; Zhao, Y.; Jiang, L. Low-Cost, Thermoresponsive Wettability of Surfaces: Poly(N-isopropylacrylamide)/Polystyrene Composite Films Prepared by Electrospinning. *Macromol. Rapid Commun.* **2008**, *29*, 485−489.

(19) Kim, E.; Xia, Y.; Zhao, X. M.; Whitesides, G. M. Solvent-assisted Microcontact Molding: A Convenient Method for Fabricating Three-Dimensional Structures on Surfaces of Polymers. *Adv. Mater.* **1997**, *9*, 651−654.

(20) Furstner, R.; Barthlott, W.; Neinhuis, C.; Walzel, P. Wetting and Self-Cleaning Properties of Artificial Superhydrophobic Surfaces. *Langmuir* **2005**, *21*, 956.

(21) Otten, A.; Herminghaus, S. How Plants Keep Dry: A Physicist's Point of View. *Langmuir* **2004**, *20*, 2405.

(22) Zhou, Q.; Wang, S.; Fan, X.; Advincula, R. Living Anionic Surface-Initiated Polymerization (LASIP) of a Polymer on Silica Nanoparticles. *Langmuir* **2002**, *18*, 3324−3331.

(23) Lvov, Y.; Decher, G.; Mohwald, H. Assembly, Structural Characterization, and Thermal Behavior of Layer-by-layer Deposited Ultrathin Films of Poly(vinyl sulfate) and Poly(allylamine). *Langmuir* **1993**, *9*, 481−486.

(24) Estillore, N.; Advincula, R. Stimuli-Responsive Binary Mixed Polymer Brushes and Free-Standing Films by LbL-SIP. *Langmuir* **2011**, *27*, 5997−6008.

(25) Fujie, T.; Park, J.; Murata, A.; Estillore, N.; Tria, M.; Takeoka, S.; Advincula, R. Hydrodynamic Transformation of a Freestanding Polymer Nanosheet Induced by a Thermoresponsive Surface. *ACS Appl. Mater. Interfaces* **2009**, *1*, 1404−1413.

(26) Ogawa, T.; Ding, B.; Sone, Y.; Shiratori, S. Super-hydrophobic Surfaces of Layer-by-Layer Structured Film-Coated Electrospun Nanofibrous Membranes. *Nanotechnology* **2007**, *18*, 165607.

(27) Estillore, N.; Advincula, R. Free-Standing Films of Semi-fluorinated Block Copolymer Brushes from Layer-by-Layer Polyelectrolyte Macroinitiators. *Macromol. Chem. Phys.* **2011**, *212*, 1552−1564.

(28) Feng, L.; Li, S.; Li, Y.; Li, H.; Zhang, J.; Zhai, J.; Song, Y.; Liu, B.; Jiang, L.; Zhu, D. Super-Hydrophobic Surfaces: From Natural to Artificial. *Adv. Mater.* **2002**, *14*, 1857.

(29) Efimenko, K.; Genzer, J. Recent Developments in Super-hydrophobic Surfaces and Their Relevance to Marine Fouling: A Review. *Biofouling* **2006**, *22*, 339−360.

(30) de Leon, A.; Pernites, R.; Advincula, R. Superhydrophobic Colloidally Textured Polythiophene Film as Superior Anticorrosion Coating. *ACS Appl. Mater. Interfaces* **2012**, *4*, 3169−3176.
(31) Ahn, B. K.; Sung, J.; Li, Y.; Kim, N.; Ikenberry, M.; Hohn, K.; Mohanty, N.; Nguyen, P.; Sreeprasad, T. S.; Kraft, S.; Berry, V.; Sun, X. Synthesis and Characterization of Amphiphilic Reduced Graphene Oxide with Epoxidized Methyl Oleate. *Adv. Mater.* **2012**, *24*, 2123−2129.